Analysis of Piles in Residual Soil from Granite Considering Residual Loads

António Viana da Fonseca, Jaime Alberto dos Santos, Elisabete Costa Esteves, Faiçal Massad

Abstract. The paper deals with the analysis of static loading tests carried out in 3 different types of piles: bored piles with temporary casing, continuous flight auger, CFA, piles (bored and CFA piles with circular section - nominal diameter Ø600 mm) and driven piles (with square section - width 350 mm). These piles were installed in the CEFEUP/ISC'2 experimental site, located in the Campus of the Faculty of Engineering of the University of Porto (Portugal), in a contact zone between the gneissic rocks and the granite mass. After a brief geological and geotechnical site characterization, the paper presents a detailed description of the piles and the instrumentation installed in two of them. Previous analyses of the test data are summed up, emphasising the difficulties in determining the residual loads resulting from the installation processes and the unloading and the reloading cycles applied to the static loading tests. This paper aims to quantify these locked-in toe residual loads, using a mathematical model - the Modified Two Straight Lines Method (MDRM) - that allows the interpretation of the pile head load-settlement curve and the determination of the shaft and toe resistances, apart from the toe residual loads. For the shaft and toe resistances, the MDRM led to consistent results with those inferred from both, the previous analysis and the extensometer measurements; the ultimate unit shaft resistance was estimated in 60 kPa. As far as the toe's residual loads are concerned, the estimated values of about 150 kN for the bored piles were also consistent with those measured but very different from that guessed in previous analysis, about 300 kN. For the driven pile, this paper arrived at an upper bound of 500 kN for the residual load and a lower bound of 60 kPa for the ultimate unit shaft resistance.

Keywords: piles, capacity, residual loads, mathematical model, saprolitic soils.

1. Introduction

In the north-western region of Portugal residual soils from granite are dominant. The thickness of these regional saprolitic soils may some times attain more than 20 m, with more common values of 5 to 10 m. The current design practice of bored and driven piles in residual weathered formations is merely semi-empirical and based on bearing capacity analysis (in general, without deformation analysis). Fully instrumented pile load tests are very much informative for the elaboration of specific correlations between load-deformation behaviour and in situ tests results, for establishing well-based design criteria.

In the Fall of 2003, the Faculty of Engineering of the University of Porto (FEUP) and the High Technical Institute of the Technical University of Lisbon (ISTUTL) invited the international geotechnical community to participate in a prediction event on pile capacity and pile load-movement response to an applied loading sequence. The event was organized by FEUP and ISTUTL in collaboration with the Portuguese Geotechnical Society, TC16 and TC18 of the ISSMGE and the organizers of the ISC'2 Conference in Porto in September 2004. A very extensive site characterization had been held, including a large variety of in situ tests in order to develop an International Prediction Event (Class A) of Bored, CFA and Driven Piles. Researchers and designers were invited to deal with this investigation results in order to predict the real response of the pile foundations. Several in-situ testing techniques were used - SPT, CPT and CPTU, PMT and DMT; Seismic: Cross-Hole (CH) and Down-Hole (DH). Undisturbed samples were recovered and an extensive laboratory-testing program was carried out: oedometric consolidation tests, CK_0D triaxial tests using local strain measuring devices and bender-extender elements, as well as resonant column tests. In December 2003, a total of 33 persons from 17 countries submitted predictions. Static loading tests were then performed. A summary of the capacity predictions and the static loading tests has been published by Santos *et al.* (2005, 2006) and a more detailed report in Viana da Fonseca & Santos (2006). This paper presents the steps involved in preparing the international pile prediction event, the analysis of the relevant test data, and the results of the predictors' efforts.

Three different kinds of piles were executed: bored piles with temporary casing, continuous flight auger, CFA, piles (bored and CFA piles with circular section - nominal diameter Ø600 mm) and driven piles (square section with 350 mm width). For the former types, a hydraulic rotary rig

António Viana da Fonseca, Associate Professor, Faculty of Engineering, University of Porto, Rua Dr. Roberto Frias, 4200-465 Porto, Portugal. e-mail: viana@fe.up.pt.
Jaime Alberto dos Santos, Assistant Professor, High Technical Institute, Technical University of Lisbon, Av. Rovisco Pais, 1049-001 Lisboa, Portugal.
e-mail: jaime@civil.ist.utl.pt.
Elisabete Costa Esteves, MSc Assistant School of Engineering, Polytechnic Institute of Porto, Rua de S. Tomé, Porto. e-mail: efm@iscp.ipp.pt.
Faiçal Massad, Professor, Polytechnic School, University of São Paulo, Av. Prof. Almeida Prado 271, Trav. 2, Cidade Universitária, 05508-900 São Paulo, SP, Brasil.
e-mail: faical.massad@poli.usp.br.
Submitted on August 8, 2006; Final Acceptance on January 26, 2007; Discussion open until August 31, 2007.

on a base machine, allowed a temporary casing, installed by jacked and rotary crowd system, followed by a dry concretion, while, in CFA, an injection of concrete (slump of 190 mm) with a pressure of 6 MPa at the beginning, was made while pulling out the auger. The equipment used for driving the precast piles was a 40 + 10 kN hydraulic hammer, falling from about 23 cm, mounted on a base machine.

Although the results of these tests have already been analysed elsewhere (Viana da Fonseca *et al.*, 2004, 2006, Santos *et al.*, 2005, 2006, Costa Esteves, 2005; Fellenius *et al.*, 2007), in this paper a different approach is described taking into account the residual loads resulting from the installation process and loading cycles.

This work aims to quantify these toe residual loads, using a mathematical model developed from the Cambefort's Laws, and considering piles compressibility (Baguelin & Venon, 1972) and the residual loads and the inversion of the balanced negative shaft load (Massad, 1992, 1995). Based on this model, methods of analysis of the pile head load-settlement curve were developed allowing the identification of the shaft and base resistances, apart from the toe residual loads.

2. Site Characterization

As described elsewhere (Viana da Fonseca *et al.*, 2004, 2005, 2006, detail diverse aspects of this rich and specific profile), the CEFEUP/ISC'2 experimental site is located in a contact zone between the gneissic rocks and the granite mass. The type of regional transition between the two bodies is not a single discontinuity surface but a gradual one, consisting of an eastward "probabilistic" decreasing of feldspar bands maintaining the geological planar anisotropy, with constant strike and dip, but with frequent zones of abrupt lithologic changes. The weathering process tends to transform the feldspar into kaolin mainly in the geological contact zones where namely later fluid weathering action was more intense. Typical Porto granite is a leucocratic alkaline rock, medium to coarse grained, with mega-crystals of feldspars and two micas.

A detailed experimental work was carried out in order to characterize the extent of the weathered profile. The tests layout is presented in Fig. 1 (Viana da Fonseca *et al.* 2004).

Apart from the natural spatial variability of the structure and fabric of these residual soils due to some preserved relic heritage, there is evidence of a fairly homogeneous pattern of ground profile in geotechnical terms, as demonstrated by the results obtained with continuous sampling taken from drilling, with the SPT sampler and from high quality samplers. The former are shown in Fig. 2. Their description is presented schematically in this figure, including photos of samples obtained from borehole S3.

The first stage of the site characterization included 4 SPT, 5 CPTU, 5 DMT, 3 PMT and several CH, DH, SASW and CSWS, while in the second stage 4 CPTU and 4 DMT were performed. The technical data of the first stage of in

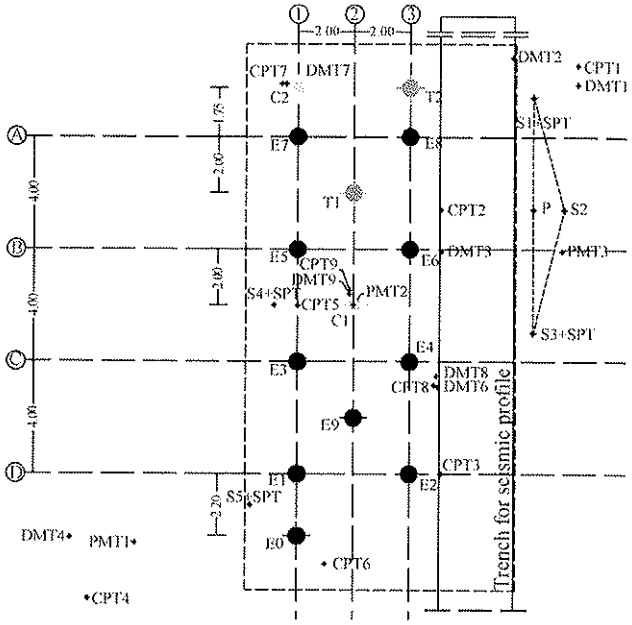

Figure 1 - Layout of the site characterization activities (including location of the piles).

situ tests is summarized in Fig. 2 (above) as well as in the forecoming Fig. 3. Other results can be found in Viana da Fonseca *et al.* (2006).

The results of grain size analyses show that both clay and silt particles decrease with increasing depth, whereas sand particles increases with depth. Kaolinite is the main mineral in the clay fraction (details in Viana da Fonseca *et al.*, 2006).

Undisturbed samples were carefully taken from the experimental site, in boreholes at specific depths, using high quality piston samplers - Shelby, Mazier and T6S-Triplex (Viana da Fonseca & Ferreira, 2002). The laboratory tests conducted in the first phase of the programme, comprised 6 CK0D triaxial - 4 in compression with bender element (BE) readings and 2 in extension - with local strain measurements, 2 resonant column tests (RC), and 1 oedometer test. A general overview of the obtained results is presented in Viana da Fonseca *et al.* (2006).

A first insight to these tests results, pointed out the following strength parameters: $\phi' = 45.8°$; $c' = 4.5$ kPa. At rest coefficient K_o was taken as 0.50. Regional experience indicates even lower values (Viana da Fonseca & Almeida and Sousa, 2001, Viana da Fonseca, 2003).

3. Piles Description

3.1. Types of installed piles

In the experimental site, 3 different kinds of piles were executed: 600 mm O.D. diameter bored piles ("E"-piles) installed using a temporary casing, 600 mm O.D. diameter augered (CFA) piles ("T"-piles) and 350 mm diam-

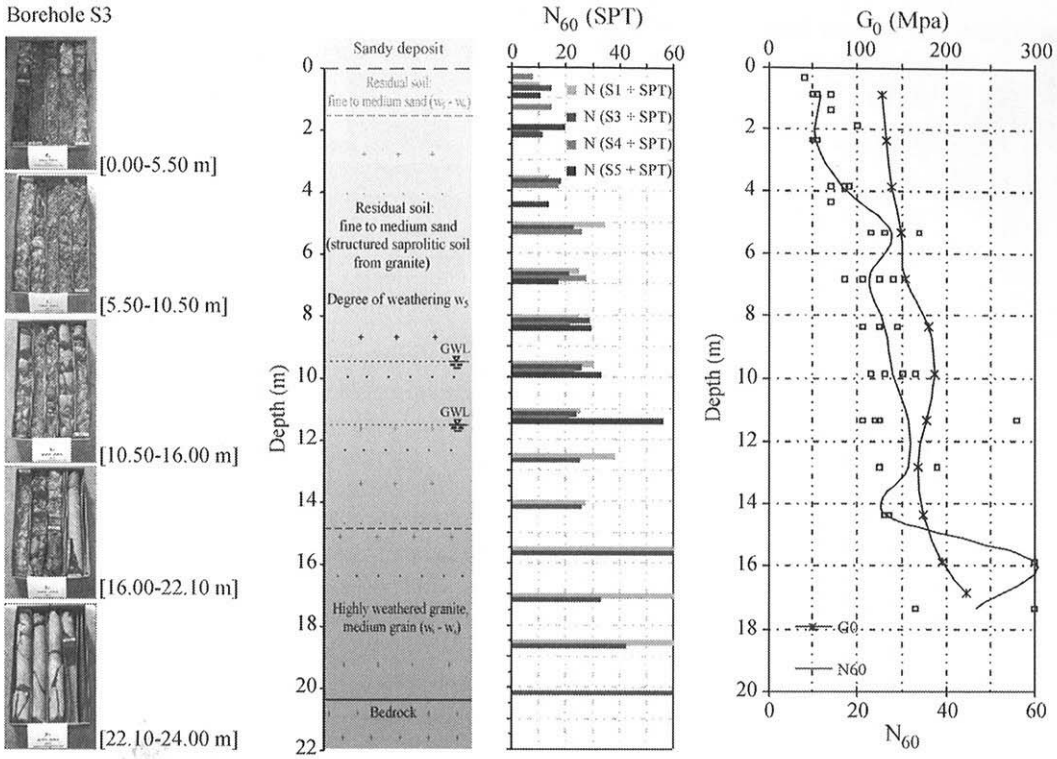

Figure 2 - Geotechnical profile with photos taken from samples obtained in borehole S3; N_{60} results in depth with average shear modulus G_0 from CH shear waves, across two different sections: S2-S1 & S3-S2.

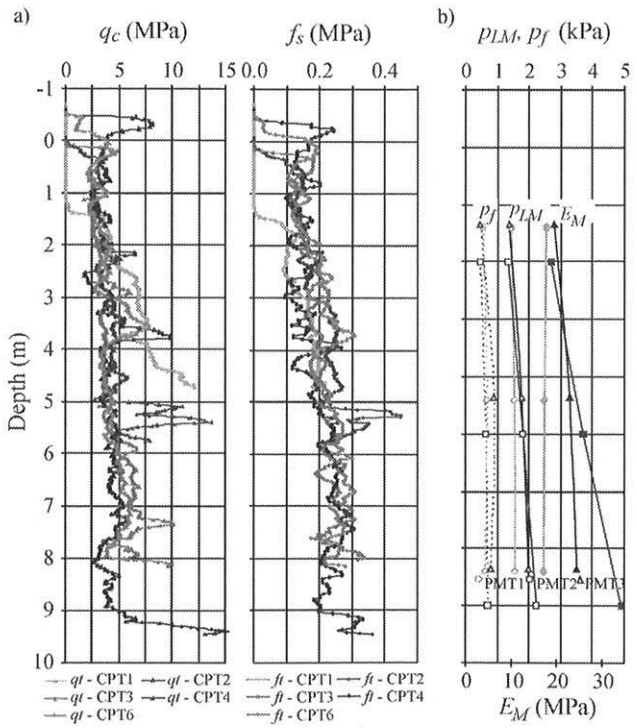

Note: pore pressures measurements (u_2) are zero: it is reasonable to consider $q_c \cong q_t$ and $f_s \cong f_t$.

Figure 3 - *In-situ* tests profile: a) CPTU: q_c and f_s; b) PMT: p_f, p_{LM} and E_M.

eter square, driven, precast concrete piles ("C"-piles). For the former types, a hydraulic rotary rig on a base machine, allowed a temporary casing, installed by jacked and rotary crowd system, followed by a dry concretion, while, in CFA, an injection of concrete (slump of 190 mm) with a pressure of 6 MPa at the beginning was made while pulling out the auger. The equipment used for driving the precast piles was a 40 + 10 kN hydraulic hammer, falling from about 23 cm, mounted on a base machine. These 3 different types of piles were loaded axially side by side up to failure (piles E9-bored, T1-CFA and C1-driven). The location of the piles is represented in the layout map (Fig. 1).

The C-piles, were driven on September 17, 2003 with a 40 kN drop hammer. In January 2004, Pile C1 was subjected to a static loading test (Fig. 4).

The E-piles, namely the one denoted by E9, were constructed in August 2003 by first using a rotary drilling rig to install a temporary casing that was cleaned out using a 500 mm cleaning bucket (Fig. 5). The external diameter of the cutting teeth at bottom of the temporary casing was 620 mm. The concrete was placed by using a drop chute in the water-filled casing. Concrete slump was 180 mm and concrete "over-consumption" was below 10%. The casing was withdrawn on completion of the concreting. In January 2004, Pile E9 was subjected to a static loading test.

The T-piles, namely the one denoted by T1, were constructed in August 2003 using a rotary drilling rig and a 600 mm continuous flight auger with a 125 mm I.D. stem.

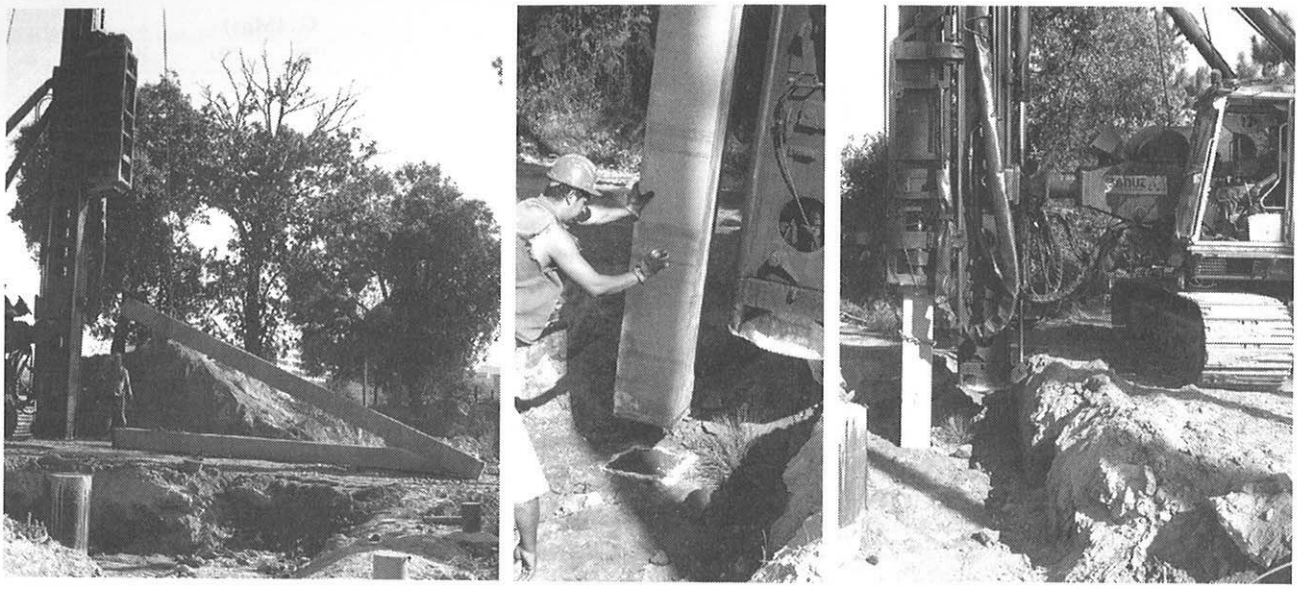

Figure 4 - Sequence of the execution tasks for the precast concrete driven piles.

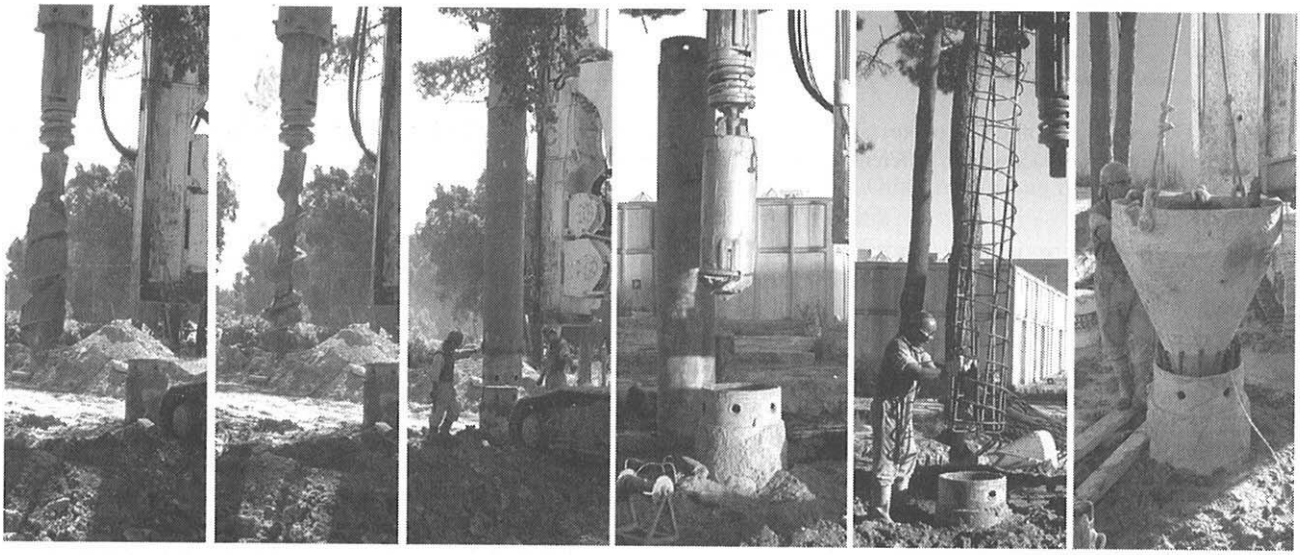

Figure 5 - Sequence of the execution tasks for the bored piles with temporary casing.

The maximum torque of the rotary head was 120 kNm and the pull-down force was 45 kN. The auger penetration rate was approximately 25 mm/s. The concrete grout was ejected with a 6 MPa pressure at the beginning of the grout line and a steady concrete flow of 700 L/min (Fig. 6). Concrete slump was 190 mm and concrete "over-consumption" was 6%. In January 2004, Pile T1 was subjected to a static loading test.

3.2. The static pile load tests (SPLT) - Instrumentation

The 3 different kinds of piles were loaded axially by static test in utmost similar ground conditions since they were conducted in close proximity. The location of the piles was shown in Fig. 1 and the layout of the testing area is disposed in Fig. 7, together with photos of the testing assembling. Information about the piles were provided to the predictors as:

- 10 bored piles (E0 to E9, with a circular section of 600 mm in diameter). The drilling equipment was a Soilmec R-620 hydraulic rotary rig mounted on a Caterpillar 3.30C base machine; temporary casing installed by jacking and rotating crowd system;
- 2 CFA piles (T1 and T2, with a circular section, 600 mm in diameter). The drilling equipment: was a Soilmec R412 HD rotary drilling rig;
- 2 driven piles (C1 and C2, square section with 350 mm width). The drilling equipment was a Banut 40 + 10 kN hydraulic hammer mounted on an Akerman H14B base machine.

The bored piles E1 to E8 piles with 22 m of embedded length were built for reaction purposes. All the others are short piles with 6 m of embedded length.

The static pile load tests (SPLT) were performed following the recommendations of ERTC3-ISSMGE (De Cock *et al.*, 2003) and ASTM DI 143-81. For each loading

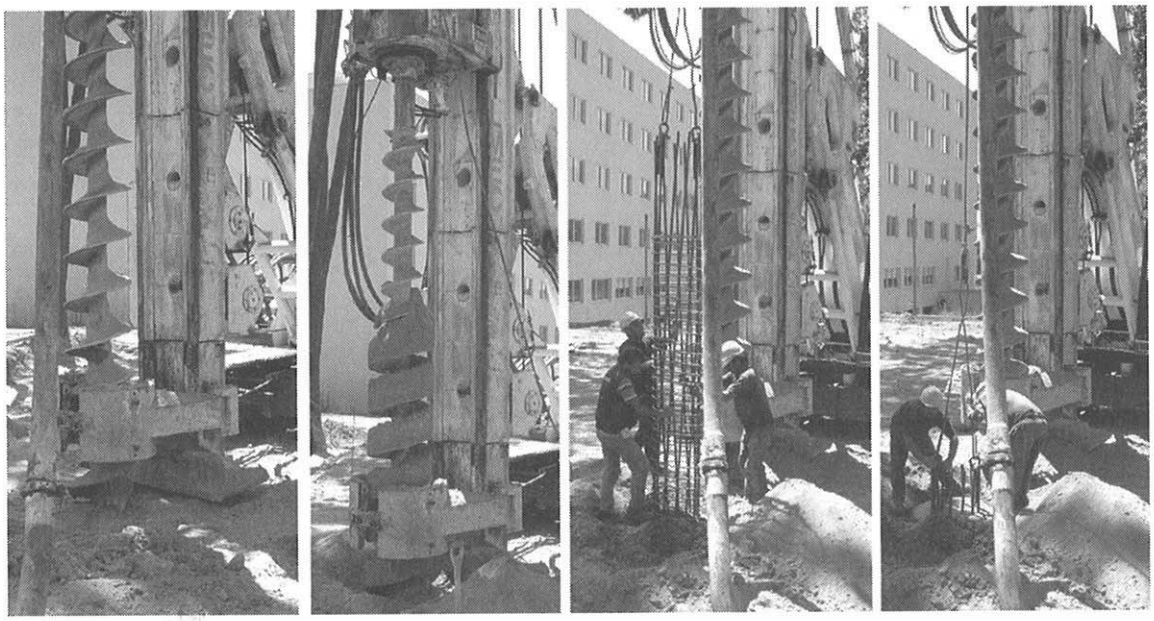

Figure 6 - Sequence of the execution tasks for the CFA piles.

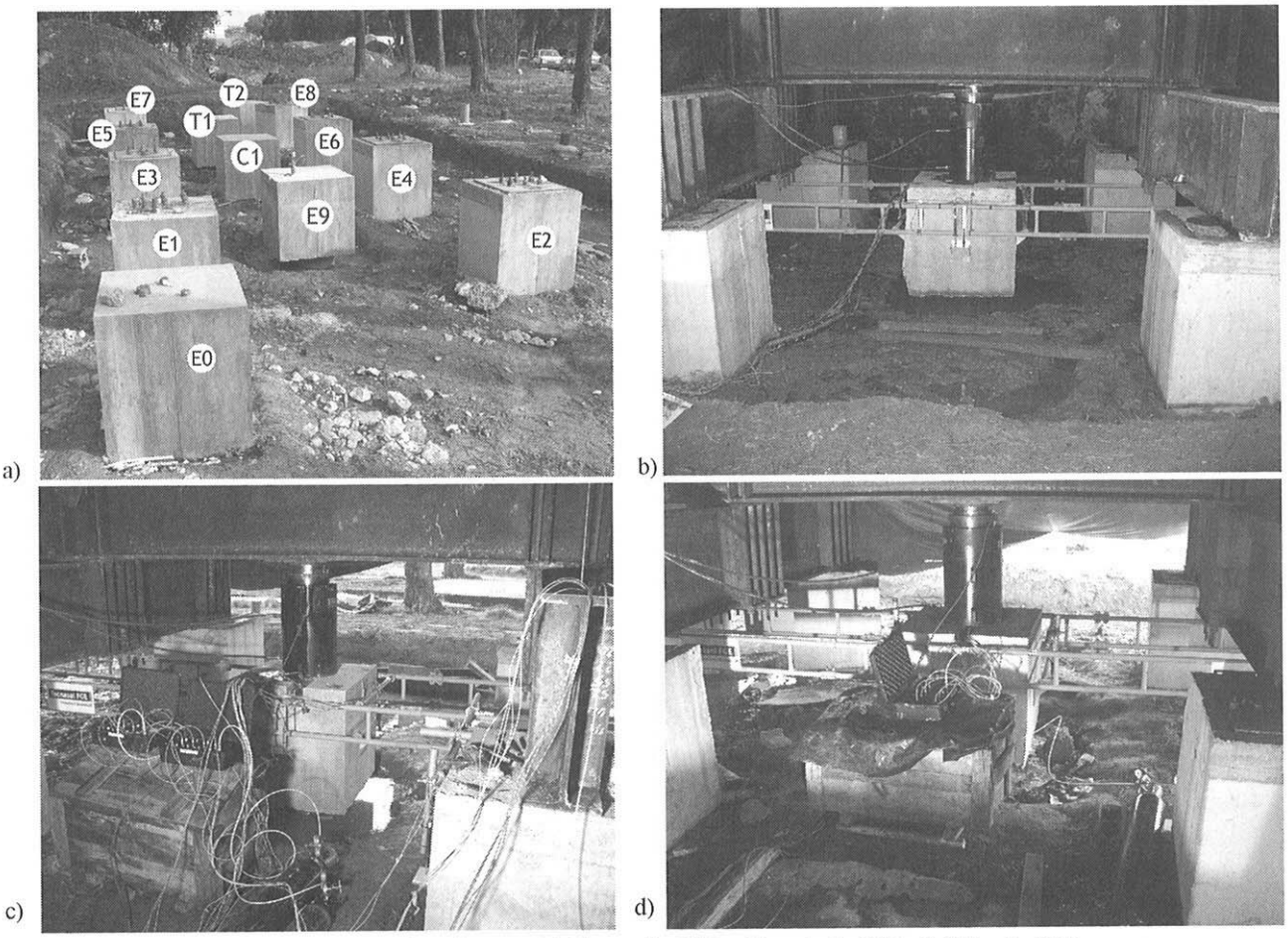

Figure 7 - a) Layout of the experimental site; pile tests: b) driven pile (C1); c) bored pile (E9); d) CFA pile (T1).

stage the load was maintained until the displacement rate became less than 0.3 mm/h, with a minimum of 0.5 h and a maximum of 2 h.

Each of Piles E9 and T1 was instrumented with six retrievable Geokon extensometer Model A9 anchors, placed in a PVC pipe centrically cast in the pile at 1,020 mm spacing with the first anchor 150 mm below the pile head. The lowest anchor was 750 mm above the pile toe. The positions of the extensometer anchors in Piles E9 and T1 are shown in Fig. 8. In pile T1 there is similar pattern.

The instrumentation provides the change of length (shortening) between each anchor and the lowest anchor (Anchor #6) as induced by the load applied in the static loading test. A shortening between anchor points divided by the length between the points corresponds to the average strain over that distance. The use of retrievable extensometer instrumentation does not allow residual loads to be measured; these may assume substantial values in driven piles, but also non-negligible levels in cast-in-situ piles (Fellenius 2002a, 2002b).

In addition to the anchors, a 350 mm diameter flat-jack load cell was placed between two 25 mm thick, 450 mm diameter steel plates in Pile E9. The load cell was connected to the bottom of the rebar cage and lowered with the cage into the pile before grouting. The operating pressure range of the load cell ranged from zero through 20 MPa (Fellenius *et al.*, 2007). The cell pressure measured in the static loading test multiplied with the pile cross sectional area was assumed to correspond to the portion of applied load reaching the pile toe. However, after the loading tests had been completed, the piles were extracted and inspected and the following was detected: while the pile surfaces were smooth and measurements of the actual diameter of Pile E9 showed it to range from 611 mm through 605 mm, *i.e.*, only marginally larger than the nominal 600 mm diameter, the measurement of the diameter at the pile toe show that, starting at about 0.5 m above the pile toe, the diameter had reduced conically toward the toe to a value of about 525 mm. Figure 9 shows a photo of the extracted pile and load cell.

The validity of the assumed conversion from cell pressure to load is questionable. It is likely that the stress in the donut-shaped concrete zone outside the load-cell will experience a stress that is different to that of the pressure inside the load cell, and, therefore, the pile toe load determined from the load-cell pressure would be under- or over-estimating the load at the pile toe to variable and unknown degree in the test. Confirming the mentioned uncertainty with the toe loads determined from the toe-cell pressure, the loads in Pile E9 determined from the strain measurements in the pile are not in perfect agreement with the toe-cell values by any assumed pile diameter. This is debated in the analyses presented in what follows.

3.3. Structural materials (reinforced concrete) properties

The prediction of the behaviour of the piles subjected to compression loads is conditioned by the pile structural

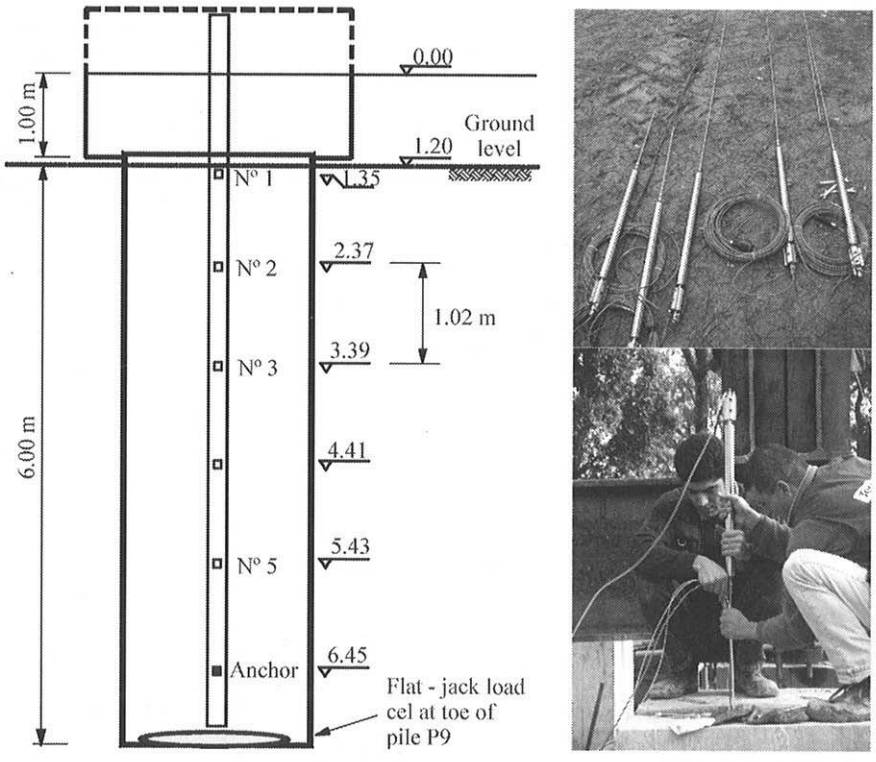

Figure 8 - Positions and illustration of extensometers anchors in Pile E9 and load cell (Fellenius *et al.* 2007).

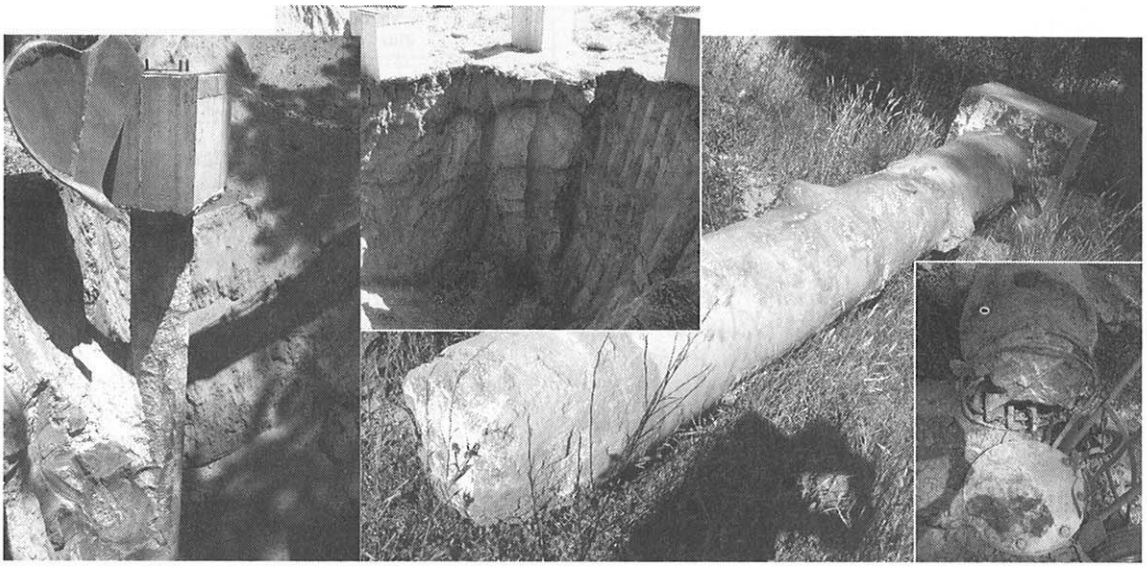

Figure 9 - Photo of Pile E9 after extraction with detail of the pile toe and load cell after it was removed from pile (Costa Esteves, 2005).

material - reinforced concrete. This has leaded to a careful evaluation of the mechanical properties (with emphasis to the Young's modulus) of the reinforced concrete, differently manufactured and disposed in the three classes of piles. While the reinforcing steel is - for its industrial reproducibility - very much stable in its properties, the concrete is not. This is obviously associated to its variable composition in manufacturing and the moulding process and the ambient conditions during the execution of piles.

For this reason, while the properties of the precast concrete (for the driven piles) were faithfully accepted (see Table 1 in paragraph 6.1), in the bored and augered piles this has demanded some steps and constitutive evaluations, as described in what follows.

Several cubic specimens, taken for the occasion of the placement of the concrete, were tested by standard processes and the "characteristic" compression strength was calculated by usual processes, taking into account the necessary statistic coefficients. The values obtained for each group of piles for this average resistance (deduced from the characteristic) were 35,7 MPa, for the bored, and 49 MPa, for the augered. This has allowed for a first determination of the Young modulus, by applying correlative equations proposed by the European codes. Values obtained for the three classes were 30.8, 36.1 and 36.3 GPa, for the bored, augered and driven piles, respectively.

In doubt with this indirect evaluation of the modulus, taken from the correlation with the compression strength, compression tests with local and precise instrumentation were executed with rotary cored specimens, taken from the tested piles, and different values were attained, especially for the bored and augered piles: 20.0 GPa and 39.2 GPa, respectively.

This was at first time surprising, mostly because of the very much lower value obtained from these thorough and rigorous tests in the bored piles. It should, however, be denoted that there is a singular pattern of the stress-strain response, which reveals a lower stiffness in the low levels of induced stress that is attributed to the poorer quality of the "concrete was placed by using a drop chute in the water-filled casing", in the "E-piles". This is not observed in the "grout concrete that was ejected with high pressure" in the "T-Piles". This concrete is, by being prepared with better aggregates and a chemical additive for decreasing its viscosity, composed with a smaller percentage of water, which endows a smaller void ratio, resulting in a more stable and dense micro-structure. On the other side, the less controlled concrete and the eventual air-inducting deposition method on the bored piles, has created a softer material, which may be also more sensible to the less effective curing conditions in the most superficial layers, in a warm climate.

Weaker concretes are also more sensible to the time factors (creep) than the high quality ones. Being the static pile test loading steps sustained for a relevant period (between 1/2 to 2 h), they are very different of the transient condition of the coring specimens tested in laboratory, tested in very rapid cycles. This has been proved in creeping tests over different classes of concretes.

For all what has been said, the surprising differences in the Young modulus between the bored and augered piles can be justified. In the back-analysis made with the extensometer measurements this may - and will - be expressed.

4. Results of the Static Pile Load Tests (SPLT)

Pile C1 was loaded in increments of 130 kN with two early unloading cycles. When a total load of 1,300 kN had been reached at a pile head movement of 4.9 mm, the pile movement increased progressively (Fig. 10). A maximum

load of 1,500 kN was reached at a total movement of 50 mm, beyond which the movement continued for a slightly decreasing load.

Piles E9 and T1 were loaded in increments of 150 kN. The loading sequence was in cycles to 300 kN followed by unloading, to 600 kN followed by unloading, and to 900 kN followed by unloading, whereafter the piles were loaded to maximum loads of 1,350 kN and 1,200 kN, respectively (Fig. 10). For both Piles E9 and T1, the movement at 1,200 kN applied load was 100 mm, *i.e.*, 17% of the pile head diameter.

This driven pile C1, although having a smaller cross-section (43.3% of the others) has shown a stiffer response than piles E9 and T1. This is a clear indication that the installation effects play a crucial role in pile behaviour. In this case, the pile driving process may have induced a significant increase of the horizontal stresses in the surrounding soil, as well as some densification. For piles E9 and T1, the ultimate resistance cannot be clearly defined - Fig. 10.

The ultimate pile capacity for the driven pile C1 was reached for a relative settlement of about 10%. This value seems to be in good agreement with recent studies in centrifuge tests with displacement piles in sands (Fioravante *et al.*, 1995).

On the other hand, for the "non-displacement" piles E9 and T1, even for a relative settlement of about 25%, the ultimate resistance was not reached.

The five extensometers measuring shortenings over the 1,020 mm distance allowed the determination of the pile stiffness ES (Fellenius *et al.*, 2007). This was performed by means of the tangent modulus approach (Fellenius 1989, 2001). Values of 20 GPa and 40 GPa - almost equal to those deferred from the compression tests on rotary cored specimens (see above) - were obtained under the assumption that the pile diameter is equal to the nominal 600 mm value. These figures are in close agreement with the results obtained in the tests over the concrete samples, as described above.

Figures 11 and 12 shows the evolution of the load distribution for shaft and base components obtained from the extensometers during the 5th cycle of the static loading tests on piles E9 and T1. The measurements were extrapolated (dashed lines) to estimate the base load. It is clear from this

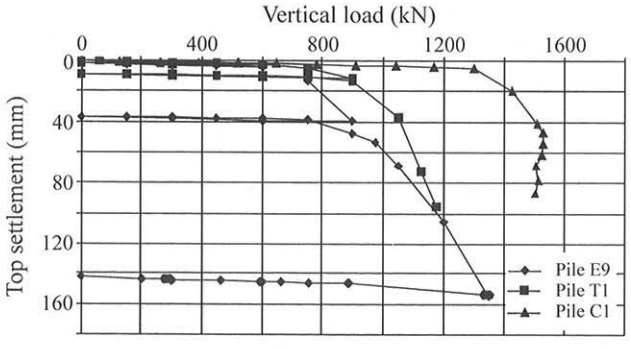

Figure 10 - Load-settlement curves from static load test.

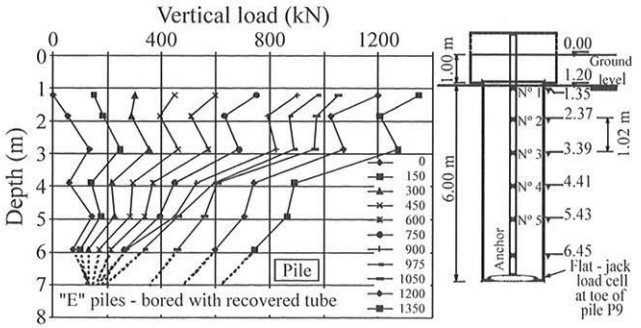

Figure 11 - Load distribution - measured in the 5th cycle of loading.

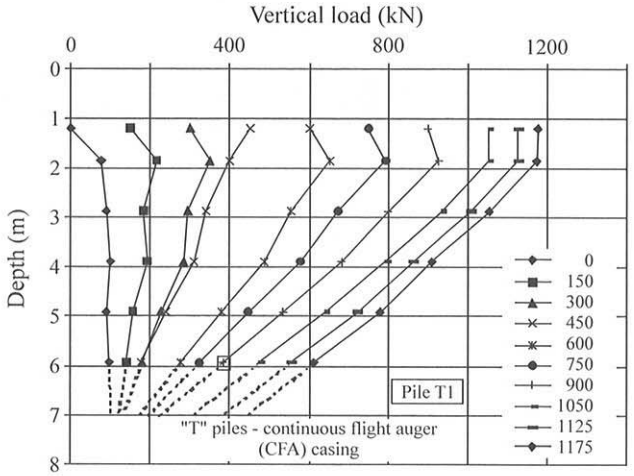

Figure 12 - Load distribution - measured in the 5th cycle of loading.

figure the progressive increase of the base resistance. For the last stages the load increments at the top and at the base are almost equal. It can be concluded that while the ultimate shaft resistance was reached, the base resistance was not fully mobilised. It is also noticeable the presence of residual loads in the beginning of the loading.

Another interesting analysis, as referred above, was the comparative evaluation of the performance of the load cell installed in the bored pile (E9), by taking an area correction or not, and the one deduce from the extensometers. This is relevant as the pile toe of extracted Pile E9 show that, starting at about 0.5 m above the pile toe, the diameter had reduced conically toward the toe to a value of about 525 mm (Fig. 13 includes also a photo of the extracted pile and load cell).

As it is clear from the picture, the correction of the area is essential for the adjustment (mainly at higher loads), taking the values derived from the extensometers to converge to the values of the corrected cell area.

5. Summary of Previous Analysis of the Results of the SPLT

As stated in a previous publication dealing with these results (Fellenius *et al.*, 2007), analysis of pile response to

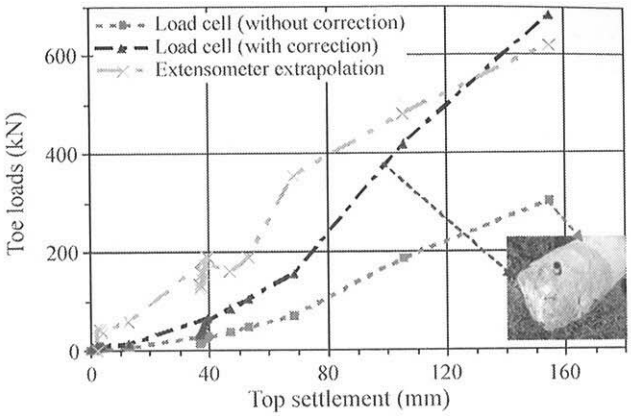

Figure 13 - Comparison of the values of the load transmitted to toe in pile E9, deduced form the load cell without and with area correction and measures from the extensometers.

load may be made from diverse of data input, namely from in situ tests, such as Standard Penetration Test (SPT), Pressuremeter Tests (PMT), Dilatometer Tests (DMT), and Cone Penetrometer Tests (CPT and CPTU). Analysis based on soil parameters determined in laboratory tests rely on simple total stress (alpha) or effective stress (beta) methods, or on more or less sophisticated numerical - finite element - methods. Most of these analyses give unreliable predictions of pile response, as it was proved by the results of ISC'2 International Pile Prediction Event in residual soil from granite (Santos *et al.*, 2005; Viana da Fonseca & Santos, 2007), this may only overcome by through calibrating of these methods from results of full-scale tests in specific geoenvironments.

Fellenius *et al.* (2007) emphasized the inadaptability of an analysis based on alpha method in these granular residual soils, being the beta-method the only adapted to their well-drained conditions. In that paper, preference was given to analysis based on CPTU data, for its continuous and representative scanning of the site spatial variations. The distinction between CPT and CPTU data is that the later includes the area correction of the cone tip resistence, q_c, for the pore pressure, U2. The Dutch method (DeRuiter & Beringen, 1979), the method of Schmertmann (1978), the LCPC method (Bustamante & Gianeselli, 1982) as quoted by the CFEM 1992, the method of Meyerhof (1976), limited to piles in sands, and the method of Tumay & Fakhroo (1981), limited to piles in clay, require input of soil type, but differentiating two soil types, "clays" and "sands". The Eslami-Fellenius method - "E-F CPTU method" - (Eslami 1996, Eslami & Fellenius 1997) differentiates in more diverse types the soil geomechanical behaviour (as calibrated by the authors), from the CPT/CPTU results, generating six soil main classes, with some intermediate materials (CFEM, 1992).

Fellenius *et al.* (2007) simulated the evolution of the load distribution in the static load test obtained in the bored pile (E9), by assuming that the base resistance would be equal to the value measured at the load cell placed at the pile toe, corrected by the ratio of areas of the cell and the 525 mm diameter pile toe as measured after excavation and extraction. It is possible, however, that the stress in the donut-shaped concrete zone outside the load-cell area may experience a stress concentration that is different from the pressure monitored by the load cell. Therefore, the "net" pile toe load derived from the load-cell pressure could be under- or overestimated by unknown degree. Moreover, the area to be used may be different during the test, from the very early stages to "ultimate" load.

From some of the previous analysis of this study, reported in Santos *et al.* (2005) and Fellenius *et al.* (2007), the following conclusions were extracted:

- extensometer measurements available in Piles E9 and T1 allowed for a very reliable estimation of load distribution ("transfer") indicating values of shaft and toe resistances, for 1,200 kN/100 mm movement, of 1,000 kN and 200 kN, and 800 kN and 400 kN, respectively, however, the piles were expected to have some residual loads, locked-in before the static loading test, as consequence of the installation process, with an unknown magnitude, since it was not determined before (the adopted monitoring system and process was not prepared to register these loads); reasonable trial-and-error analysis of the data (as expressed by Fellenius *et al.*, 2007) indicated the presence of residual loads and estimated their values; however overestimating the shaft resistance by 300 kN and consequent underestimation the toe resistance by the same amount; in fact, effective stress analysis of the data, adjusted to these residual loads correlates to a constant beta-coefficient value of 1.0 and a toe coefficient equal of 16; this toe coefficient is not in balance with the beta-coefficient, being this attributed to disturbance of the soil at the toe during the construction process;
- a back-analysis of the loading test on Pile C1 using the same 0.1 value for beta-coefficient, as that derived from the load (transfer) distribution of Piles E9 and T1, indicates total shaft and toe resistances of 520 kN and 980 kN, respectively; this toe resistance corresponds to a toe coefficient of 70, which is in balance with the beta-coefficient of 1.0;
- the compilation of submitted predictions (Santos *et al.*, 2005; Viana da Fonseca & Santos, 2007) indicates that most predictors overestimated the bored pile capacities, mostly due to an overestimation of the toe resistances, which is also expressed in the presence of residual (locked-in) loads.

6. New Analysis of the SPLT Results

6.1. Mathematical model

A new analysis was carried out with the purpose of having a more fundament evaluation of the residual loads and, consequently, the load distribution in ultimate shaft re-

sistance (A_{lr}) and tip resistance (Q_{pr}), namely for 100 mm top settlement. This was possible by applying a mathematical model that allows a back analysis of the top load-settlement curve.

A model to predict single pile performance under vertical loading was proposed by Massad (1995), which includes many aspects of load transfer phenomena, considered previously by Baguelin & Venon (1972), like pile compressibility and progressive failure. In addtion, it takes into account the eventual presence of residual stresses due to driving or subsequent cycling loadings. The solutions are analytical, in closed form, and were derived using load transfer functions based on Cambefort's Laws, accounting for the current knowledge of the shaft and tip displacements, needed to mobilize the full resistances. They may be applied to bored, jacked or driven piles subjected to a preliminary monotonic loading and/or subsequent loading-unloading cycles. The soil is supposed to be homogeneous with depth, along the entire pile shaft.

A coefficient (k) that measures the relative stiffness of the pile-soil (shaft) system was introduced and defined as follows:

$$k = \frac{A_{lr}}{K_r y_1} = 4\left(\frac{h}{D}\right)^2 \frac{BD}{E} \qquad (1\text{-a})$$

with

$$K_r = \frac{ES}{h} \qquad (1\text{-b})$$

where A_{lr} is the ultimate shaft load; y_1, the pile displacement (of a few millimeters), required to mobilize full shaft resistance (see Fig. 14); D and h are the diameter and height (or embedment in the soil) of the pile; B is a Cambefort parameter (see Fig.14); K_r is the pile stiffness; E, the modulus of elasticity of the pile material, and, S, its cross sectional area. For homogeneous soils, the coefficient k is equal to the term $(\mu h)^2$ of Randolph & Wroth model (1978). The last member of Eq. (1-a) is valid for massive piles (see the list of symbols at the end of the paper).

The model gives a further insight on pile behaviour and led to a new pile classification, with respect to k values: "short" or rigid ($k \leq 2$); intermediate ($2 \leq k \leq 8$); and "long" or compressible ($k \geq 8$).

The residual stresses can be dealt with a magnifier factor (μ):

$$\mu = 1 + \frac{P_h}{A_{lr}} \qquad (2)$$

where P_h is the residual toe load, which is in equilibrium with the residual negative shaft resistance, assumed to vary linearly with depth. Note that P_h may be treated as an increment to the shaft load: in fact, from Eq. (2) it follows $\mu.A_{lr} = A_{lr} + P_h$. In other words, A_{lr} is magnified by a factor given by μ. One advantage of using μ is that it allows taking the residual loads as shaft loads in the model.

For a first loading of a "purely" bored pile, $P_h = 0$, then $\mu = 1$. Otherwise, as $P_h \leq A_{lr}$, then $\mu \leq 2$. For floating piles, $\mu < 2$. In general, this factor, that is greater than 1, is upper bounded by the smaller value between 2 and $(1 + Q_{pr}/A_{lr})$, where $Q_{pr} = R_p.S$ is the toe load at failure (see also Fig. 15). Note that the maximum and the residual unit shaft resistances (f_u and f_{res}) are supposed to be constant along the pile. Massad (1992 and 1995) showed that it is possible to obtain μ by applying the model to the rebound curve of a pile load test.

a) General equations

For the simpler case of the toe reacting with $A = 0$, that is, with an elastic-plastic behaviour (Fig. 15), the load (P_o)-settlement (y_o) curve at pile top may be expressed by the following equations (details in Massad, 1995):

$$P_o = \mu A_{lr} \frac{\beta'_3}{z} \frac{y_o}{\mu y_1} \qquad (3)$$

$$\frac{y_o}{\mu y_1} = \left(1 - \frac{\beta'^2}{2}\right) + \frac{k}{2}\left(\frac{P_o}{\mu A_{lr}}\right)^2 \qquad (4)$$

$$\frac{P_o - \mu A_{lr}}{y_o - \dfrac{\mu A_{lr}}{2K_r}} = \frac{1}{\dfrac{1}{RS} + \dfrac{1}{K_r}} \qquad (5)$$

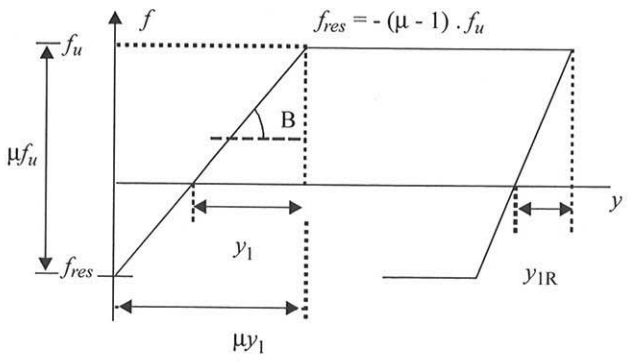

Figure 14 - Modified first Cambefort's Law.

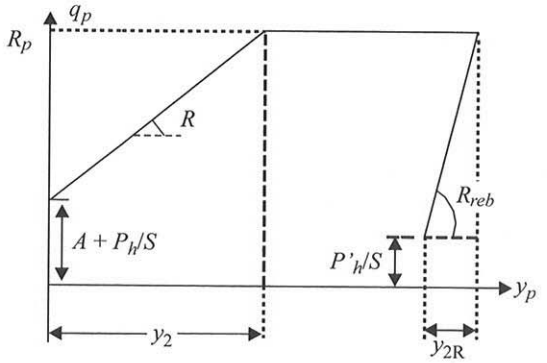

Figure 15 - Modified second Cambefort's Law.

Reporting to Fig. 16, Eqs. (3), (4) and (5) hold true, respectively, between points 0 and 3 (pseudo elastic range); 3 and 4 (progressive mobilization of shaft resistance, from top to bottom); and 4 and 5 (free development of toe resistance). Point 5 is not necessarily associated to the failure load.

The coefficient β' of Eq. (4) depends on the characteristics of the soil-pile system. For compressible piles ("long piles") $\beta' \cong 1$ and the range 3-4 turns parabolic.

For very rigid piles, this range vanishes, that is, points (3) and (4) almost coincide (Fig. 17). The other terms of Eqs. (3), (4) and (5) are defined as:

$$\beta'_3 = \frac{\tanh(z)+\lambda}{1+\lambda \tanh(z)}, \text{ with } z = \sqrt{k} \text{ and } \lambda = \frac{RS / K_r}{z} \quad (6)$$

where λ is the relative stiffness of the pile-soil (shaft and toe) system (Massad, 1995). Using the same notations of Randolph & Wroth (1978), it is possible to rewrite λ as follows:

$$\lambda = \frac{2 D G_l}{(1-\nu)\eta} \frac{1}{K_r} \frac{1}{\mu h} \quad (7)$$

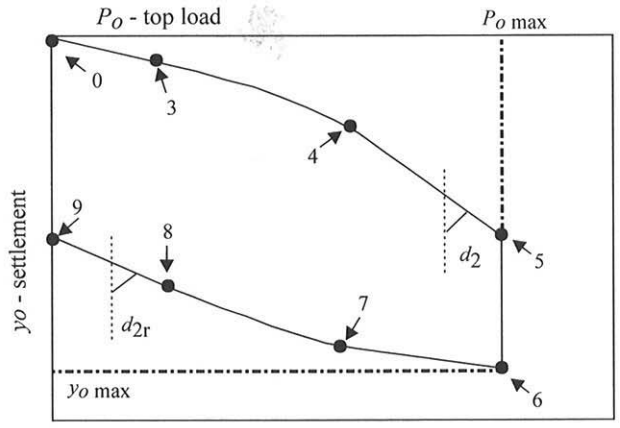

Figure 16 - Theoretical load-settlement curve of pile head for $A = 0$.

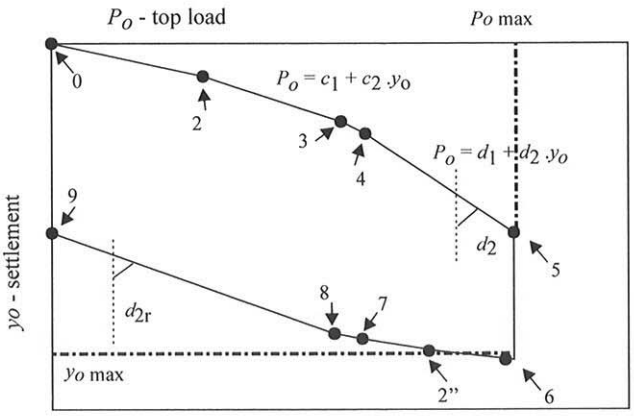

Figure 17 - Theoretical load-settlement curve of pile head for $A \neq 0$ - short piles.

where G_l is the small strain shear modulus of the soil at the pile base level; η is a correction factor to allow for the pile base depth effects and $\mu h = z = \sqrt{k}$. Here, the symbol "μ" has another meaning and must be distinguished from the magnifier factor given by Eq. (2).

Equations (3), (4) and (5) also apply to the unloading ranges 6-7, 7-8, and 8-9 (Figs. 16 or 17): it is sufficient to use the appropriate Cambefort's parameters for rebound, as shown in Figs. 1 and 2; moreover, if the loading stage ends further to point 4 (full mobilization of shaft resistance), $\mu = 2$ at $P_o = P_{omax}$ (see Massad, 1995) and Eqs. (3), (4) and (5) become:

$$P_{o\,\max} - P_o = 2 A_{lr} \frac{\beta'_3}{z} \frac{y_o}{2 y_1} \quad (8)$$

$$\frac{y_{o\,\max} - y_o}{2 y_1} = \left(1 - \frac{\beta'^2}{2}\right) + \frac{k}{2}\left(\frac{P_o}{2 A_{lr}}\right)^2 \quad (9)$$

$$\frac{P_{o\,\max} - P_o - 2A_{lr}}{y_{o\,\max} - y_o - \dfrac{A_{lr}}{K_r}} = \frac{1}{\dfrac{1}{RS} + \dfrac{1}{K_r}} \quad (10)$$

The practical application of the model includes: the understanding of the factors that control the shape of the P_o - y_o curve; the partition of load in ultimate shaft and toe resistances; the study of the rebound and its influence in the general behaviour, among others.

b) Rigid piles

For rigid or "short" piles ($k < 2$), points 3 and 4 almost coincide and the shape of P_o - y_o curve is reduced to two straight lines. Massad & Lazo (1998) proposed a very simple graphical solution, called "Two Straight Lines Method" (MDR). Later on, this method was modified by Marques & Massad (2004) to include the term $A \neq 0$ (Fig. 15), that is, assuming a rigid-elastic-plastic behaviour for the soil at the base toe of the pile. It will be mentioned here as the "Modified Two Straight Lines Method" (MDRM). The physical meaning of the term $A \neq 0$ may be explained in the following way: for some short piles, as the displacement piles, the toe reacts significantly to small displacements and an elastic bi-linear response would be more adequate than the rigid-elastic one. For simplicity, the MDRM adopted the later response.

Reporting to Fig. 17, the P_o - y_o curve may be represented by a polygonal that starts at point 0 and ends at point 9. The equations of lines 2-3 (pseudo elastic range) and 4-5 (free development of toe resistance) are, respectively:

$$P_o = \mu A_{lr} \frac{\beta'_3}{z} \frac{y_o}{\mu y_1} + A S w_2 \text{ (range 2-3)} \quad (11\text{-a})$$

with

$$w_2 = \frac{1}{\cosh(z) + \lambda \sinh(z)} \quad (11\text{-b})$$

and

$$\frac{P_o-(\mu\, A_{lr}+A\, S)}{y_o-\dfrac{\mu\, A_{lr}+2A\, S}{2K_r}}=\frac{1}{\dfrac{1}{RS}+\dfrac{1}{K_r}}\ \text{(range 4-5)} \qquad (12)$$

Based on the load test curve P_o - y_o (see Fig. 17), it is possible to derive the equation:

$$P_o=c_1+c_2 y_o \qquad (13)$$

by carrying out a linear regression for the range 2-3; as a consequence, from Eq. (11-a) the following relations will be obtained:

$$AS=\frac{c_1}{w_2} \qquad (14)$$

and

$$\mu y_1=\frac{\mu\, A_{lr}}{c_2}\frac{\beta'_3}{z} \qquad (15\text{-a})$$

or, taking into account Eq. (1-a):

$$c_2=K_r\, z\ \beta'_3 \qquad (15\text{-b})$$

Similarly, a linear regression for the range 4-5 (Fig. 17) gives rise to the following equation:

$$P_o=d_1+d_2 y_o \qquad (16)$$

From Eq. (12) it follows:

$$\frac{1}{d_2}=\frac{1}{RS}+\frac{1}{K_r} \qquad (17)$$

and

$$\mu\, A_{lr}+AS=\frac{d_1+AS\dfrac{d_2}{2K_r}}{1-\dfrac{d_2}{2K_r}} \qquad (18\text{-a})$$

As the term $AS.d_2/(2K_r)$ is practically negligible, this last equation may be simplified as:

$$\mu\, A_{lr}+AS\cong\frac{d_1}{1-\dfrac{d_2}{2K_r}} \qquad (18\text{-b})$$

Equations (14) to (18-b) are the basis of the so-called "Modified Two Straight Lines Method" (MDRM), applicable to rigid piles with $A \neq 0$ and allowing for the estimation of the terms μy_1, μA_{lr}, AS and RS.

6.2. Application to the Static Loading Tests (SPLT)

The analysis started with the bored pile (E9), simpler in its interpretation, followed by the analysis of the CFA pile (T1) and, finally, Pile C1, more complex. For Piles E9 and T1 a comparison was possible between the results of these analyses and of the available extensometer measurements installed along the piles.

Basically, the analysis comprised the following steps:

a) initially, the parameters of Eq. (13), for range 2-3, and (16), for range 4-5, were determined;

b) then, the term RS was computed by means of the Eq. (17); by this, it was also possible to determine λ (one of the terms of Eq. (6); and,

c) finally, z was computed by solving iteratively the Eq. (15-b); then, the values of w_2 (Eq. (11-b)), $A.S$ (Eq. (14)), μA_{lr} (Eq. (18-b) and μy_1 (Eq. (1)) were calculated.

Table 1 shows the values obtained for K_r in the different types of the analyzed piles.

6.2.1. Bored pile (E9)

The modeling of the bored pile (E9) was done by initially assuming that $A = 0$. Consequently, the straight line of range 2-3 (Eq. (13)) passes through the origin. The following linear regression, considering the non-accumulated settlements of all cycles of loadings, was obtained:

$$P_o=477\, y_o \qquad (19)$$

The linear regression of range 4-5, Eq. (16), was also estimated, resulting in:

$$P_o=694+4.84 y_o \qquad (20)$$

This was derived using the non-accumulated settlements of the 4th cycle of loading, together with the points of the 5th cycle, since slope of the range 4-5 ("free development of toe resistance"), defined by parameter R of Cambefort model, is considered unique.

Figure 18 shows how these equations fit the points of the 4th and 5th cycles of loading.

As it is expressed in the fizgure, $d_2 = 4.84$ kN/mm and $d_1 = 694$ kN. Applying the Eqs. (17) and (18-b) to the 4th cycle of loading, it follows $R.S$ = 4.86 kPa/mm, then $R = 17$ kN/mm and $\mu A_{lr} + AS = 696$ kN. Disregarding the influence of the 3 first cycles of loading and taking into account that E9 is a bored pile, it may be assumed $\mu = 1$ at the beginning of the 4th cycle. Therefore, A_{lr} = 696 kN and f_u = 61 kPa. An iterative calculation using Eq. (15-b), with c_2 = 477 kN, led to y_1 = 1.62 mm.

Table 1 - Pile characteristics.

Pile	Type	Diameter or width (mm)	h (m)	E (Gpa)	K_r (kN/mm)
E9	Bored pile	605	6	20	958
T1	Continuous Flight Auger Pile (CFA)	611	6	40	1,955
C1	Driven precast concrete pile	350	6	35.6	727

The linear regression for the range 4-5 of the 5th cycle of loading, considering the non-cumulative settlements, assumed the following equation:

$$P_o = 872 + 4.84 y_o \quad (21)$$

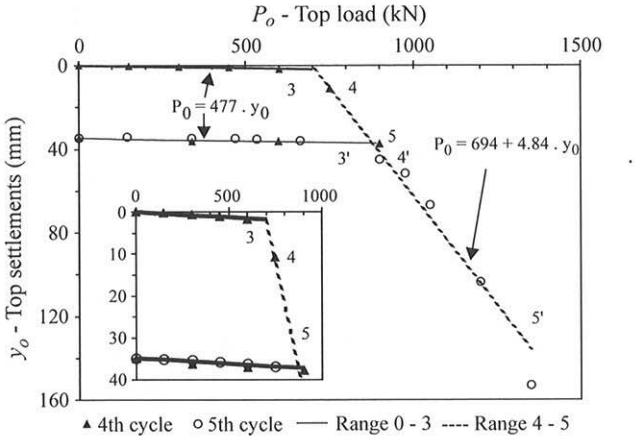

Figure 18 - Ranges 2-3 and 4-5 of 4th and 5th cycles of loadings - E9 Pile.

Observing that the slope d_2 had the same value and, with the new value for d_1, the following relation was obtained: $\mu.A_{lr}+AS = 872$ kN. Since $A_{lr} = 696$ kN and $A = 0$, then: $P_h = 872\text{-}696 = 176$ kN. Finally, the application of Eq. (2) resulted in: $\mu = 1+176/696 = 1.25$.

Note also that:

a) $k = 696/(958 \times 1.62) = 0.45 < 2$, confirming that E9 behaved as a rigid pile (Massad, 1992, 1995) (a better classification would be "very rigid");

b) $\lambda = 0.008$ (almost zero), which means that the toe contribution in terms of rigidity is very small, and,

c) in the same context, $d_2 \cong RS = 4.86$ kN/mm, since K_r value is very high (Eq. (17)).

These results are summarized in Tables 2 to 4, which include also the results of the analysis of the other two types of piles.

Figure 19 presents the measured load-settlement curves compared with the ones obtained by the application of the MDRM model, expressed by Eqs. (11) and (12).

Figure 20 is the same as Fig. 13, with the addition of the theoretical (MDRM modeled) curve, computed using $R.S = 4.86$ kPa/mm. The agreement with the toe values ex-

Table 2 - Linear regressions of ranges 2-3 and 4-5 - Static loading tests.

Pile	Range 2-3		Range 4-5	
	Linear regressions	Cycle of loading	Linear regressions	Cycle of loading
E9	$P_o = 477 y_o$	All	$P_o = 694 + 4.84 y_o$	4th and 5th
			$P_o = 872 + 4.84 y_o$	5th
T1	$P_o = 141 + 354 y_o$	2nd to 5th	$P_o = 990 + 2.13 y_o$	5th
C1	$P_o = 232 + 251 y_o$	All	$P_o = 1296 + 5.24 y_o$	5th

Table 3 - Summary of analysis results.

Pile	RS (kN/mm)	$\mu.A_{lr} + AS$ (kN)	k	AS (kN)	$\mu.A_{lr}$ (kN)	μy_1 (mm)	μ	P_h (kN)	$10^3.\lambda$
E9	4.85	696(*)	0.22	0	696(*)	1.62(*)	1.00(*)	0(*)	6.0
		872(**)			872(**)	2.03(**)	1.25(**)	176(**)	
T1	2.13	990	0.19	155	835	2.23	1.19	132	2.5
C1	5.28	1301	0.38	280	1021	1.85 to 3.64	2 to 1	509 to 0	11.7

Notes: (*) - 4th cycle of loading (**) - 5th cycle of loading.

Table 4 - Cambefort's parameters.

Pile	Shaft resistance				Toe reaction			
	B (kPa/mm)	f_{res} (kPa)	f_u (kPa)	y_1 (mm)	P_h/S (kPa)	A (kPa)	R (kPa/mm)	R_p (kPa)
E9	37.6	-16	61	1.62	0(*) 613(**)	0	17	2276
T1	32.5	-11	61	1.88	450	529	7	> 1610
C1	33.2	-61 to 0	61 to 122	1.85 to 3.64	4164 to 0	2286	43	8200 to 4033

Notes: (*) - 4th cycle of loading (**) - 5th cycle of loading.

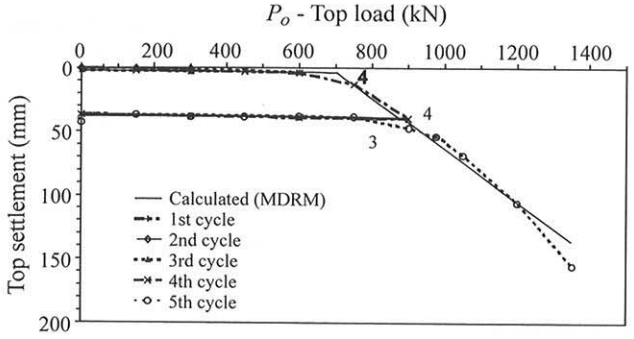

Figure 19 - Load-settlements curves from the static load test on Pile E9, with theoretical curves for the 4th and 5th cycles of loading.

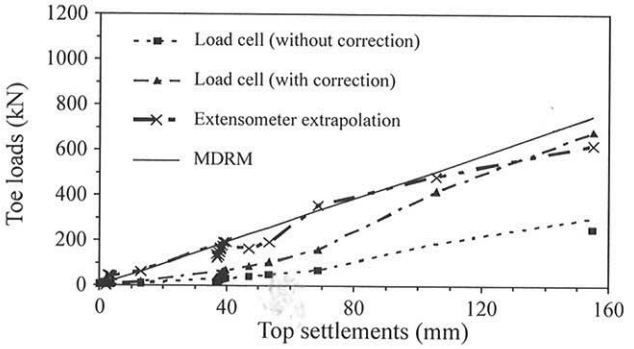

Figure 20 - Measured and computed toe loads.

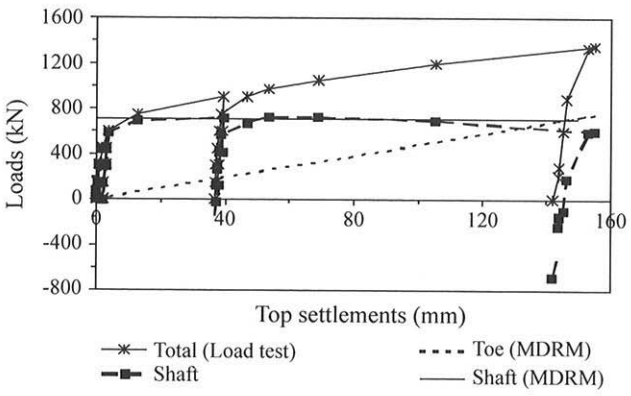

Figure 21 - Computed shaft and toe loads - E9 pile.

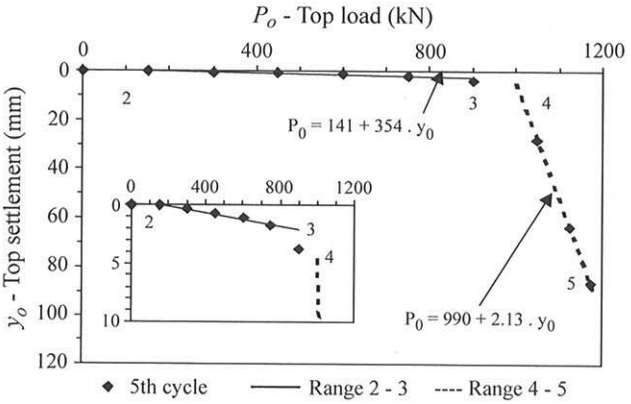

Figure 22 - Ranges 2-3 and 4-5 of the 5th cycles of loading - T1 Pile.

trapolated from the extensometers measurements is very good.

Figure 21 presents values of the shaft load, obtained by subtracting the toe component from de top load. The toe loads were computed based on the MDRM model. The dashed line corresponds to the average value of $A_{lr} = 696$ kN.

6.2.2. Pile CFA (T1)

The modeling of the curve of the CFA pile (T1) was done considering the non-accumulated values of the settlements of all cycles of loadings, except for the 1st. The following relation was obtained for the linear regression of range 2-3:

$$P_o = 141 + 354 y_o \quad (22)$$

The linear regression for the 4-5 range of the 5th cycle of loading, considering again the non-accumulated settlements, was:

$$P_o = 990 + 2.13 y_o \quad (23)$$

Figure 22 shows how these equations fit the points of the 5th cycle of loading.

As it is expressed in the graph, the range 4-5 is defined by: $d_2 = 2.13$ kN/mm and $d_1 = 990$ kN. Using Eqs. (17) and (18-b), the term $R.S$ assumed the value 2.13 kPa/mm, thus $R = 7$ kN/mm and $\mu A_{lr} + AS = 990$ kN (valid for the 5th cycle of loading). Admitting the same ultimate unit shaft resistance, derived for E9 Pile, that is, $f_u = 61$ kPa, it resulted in: $A_{lr} = 703$ kN.

From Eqs. (6) and (15-b), with $c_2 = 354$ kN/mm, it was possible to compute, iteratively, $z = 0.44$ and $y_1 = 1.88$ mm. Applying Eq. (14), with $c_1 = 141$ kN, it followed $AS = 155$ kN and therefore: $\mu A_{lr} = 835$ kN. Hence $P_h = \mu A_{lr} - A_{lr} = 835\text{-}703 = 132$ kN and, from Eq. (2), $\mu = 1 + 132/703 = 1.19$.

Similarly of what has been deduced from the analysis of the bored pile (E9), the following conclusions were obtained for the CFA pile (T1):

a) $k = 703/(1955 \times 1.88) = 0.19 < 2$, confirming that the pile is very rigid

b) $\lambda = 0.0025$, almost zero, meaning that there is a very small toe contribution in terms of stress-strain behaviour; and,

c) in this same context, $d_2 \cong RS = 2.13$ kN/mm, because K_r is very large (see Eq. (17)).

These results are, as fore mentioned, summarized in Tables 2 to 4.

Figure 23 shows the top measured load-settlement curves, compared with the computed ones, as obtained by the application of Eqs. (11) and (12).

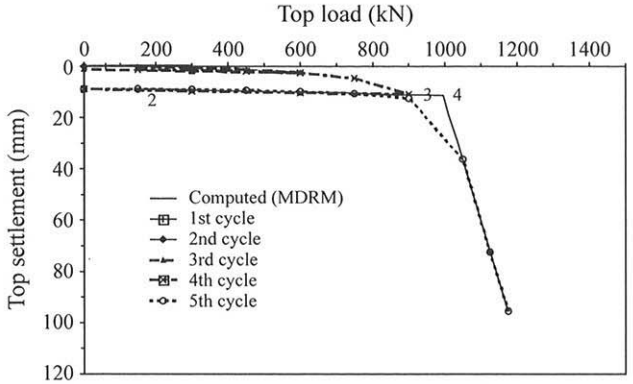

Figure 23 - Load-settlements curves from the static loading test on Pile T1, with modelled (by MDRM) curves for the 5th cycle of loading.

Figure 24 presents values of the shaft and toe loads, measured in the field. For comparison, the computed values by the MDRM are also included.

6.2.3. Precast Pile (C1)

Similarly to what had been done for the other piles, modeling of the precast pile (C1) behaviour was implemented by considering the non-accumulated values of the settlements considering together all cycles of loading. This resulted in the following relation:

$$P_o = 232 + 251 y_o \qquad (24)$$

which is really the linear regression of all points in the range 2-3.

Following the same sequence described above, the linear regression for the range 4-5 in the 5th cycle of loading was derived, taking the non-accumulated values of settlements. The results were expressed by:

$$P_o = 1296 + 5.24 y_o \qquad (25)$$

Figure 25 illustrates very clearly how these equations fit well the experimental measured points of the 5th cycle of the loading test.

With the deduced constants for the last range, d_2 = 5.24 kN/mm and d_1 = 1296 kN, it was possible to derive, from Eq. (17), $R.S$ = 5.28 kPa/mm. Therefore, the slope of the modified second Cambefort's law (Fig. 15) was obtained, R = 43 kN/mm, and consequently $\mu A_{lr} + AS$ = 1301 kN (Eq. (18-b)), valid for the 5th cycle of loading.

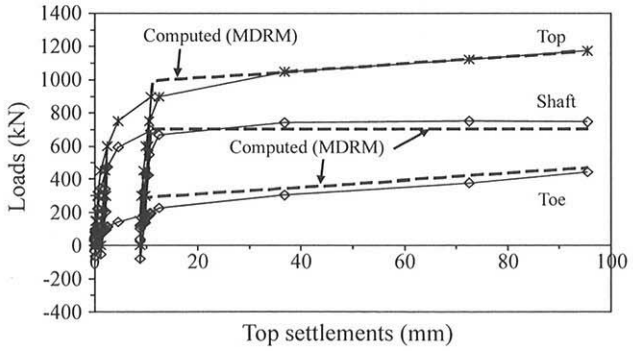

Figure 24 - Measured and computed (by MDRM) loads - T1 Pile (5th cycle).

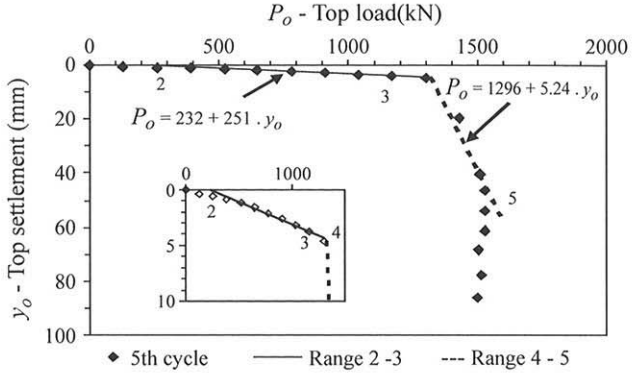

Figure 25 - Ranges 2-3 and 4-5 of the 5th cycle of loading - C1 Pile.

In the same sequence as previously described, Eq. (15-b) was solved iteratively, taking c_2 = 251 kN/mm, resulting in z = 0.62. With c_1 = 232 kN and applying Eq. (14), AS was calculated as 280 kN, resulting finally in μA_{lr} = (1301-AS) = 1021 kN and μy_1 = 3.65 mm.

The determination of μ would require more information about the load test, for example, the rebound curve, as mentioned before. Due to this fact, two extreme hypotheses had to be assumed for this pile:

a) the unit shaft resistance considered to be the same as for E9 Pile, that is: f_u = 61 kPa; consequently, A_{lr} = 512 kN, $P_h = \mu A_{lr} - A_{lr}$ = 1021-512 = 509 kN and μ ≅ 2; or,

b) being C1 a driven pile, it was reasonable to admit f_u > 61 kPa, with an upper bound given by 1021/(0,35 x 0,35 x 6) ≅122 kPa, for which $P_h = \mu A_{lr} - A_{lr}$ = 0 and μ=1.

In the same way as for bored (E9) and CFA (T1) piles, it may be concluded:

a) k = 512/(726 x 1,84) = 0.38 < 2, for μ = 2 or k = 1020/(726 x 3,65) = 0.38 < 2, for μ = 1, confirming that the driven pile (C1) is also very rigid;

b) λ = 0.012, meaning that there is a very small toe contribution in terms of rigidity; and,

c) d_2 ≅ RS = 5.28 kN/mm, since the pile is very rigid.

These results are summarized, as referred above, in Tables 2 to 4.

Figure 26 shows the results of this analysis. The computed curve, obtained by the application of the MDRM model, expressed in Eqs. (11) and (12), fits remarkably well with the observed experimental values.

6.2.4. Final comments

With these results, it was possible to evaluate the load distribution for ultimate shaft resistance (A_{lr}) and tip (toe)

Table 5 - Load distribution for 100 mm pile head settlement.

Pile	This paper			Fellenius *et al.* (2007)		
	A_{lr} (kN)	Q_p (kN)	Total load (kN)	A_{lr} (kN)	Q_p (kN)	Total load (kN)
E9 (Bored)	696	481	1177	700	500	1200
T1 (CFA)	703	499	1202	700	500	1200
C1 (Precast)	511 to 1021	1004 to 494	1515	520	980	1500

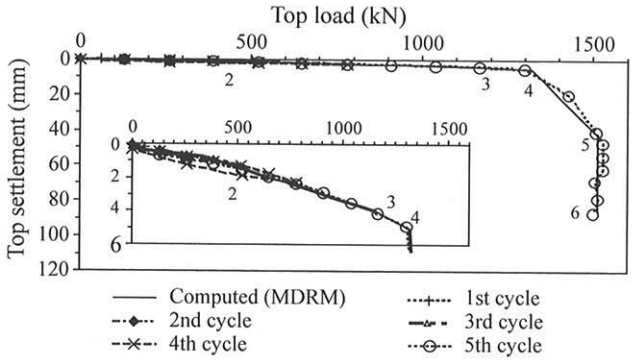

Figure 26 - Theoretical result, as modelled by MDRM, as compared with the experimental results for the 5th Cycle of Loading - Pile C1.

resistance (Q_p) levels, for a reference 100 mm top settlement, as shown in Table 5.

Derived values are in close agreement with those presented in a previous analysis, reported in Fellenius *et al.* (2007). The differences in the evaluations refer to the estimation of the residual loads. While in this paper, values derived for the bored (E9) and CFA (T1) piles were around 150 kN, Fellenius *et al.* (2007) estimated them in 300 kN. The value of 150 kN for the toe residual load is very much consistent with the measured ones indicated in Figs. 11 and 12, for E9 and T1 piles, respectively. Besides that, as far as C1 driven pile is concerned, the model that was described in this paper defined an upper bound value for residual load of 500 kN.

Assuming the validity of the hypotheses mentioned before, the ultimate unit shaft resistance for bored (E9) and CFA (T1) piles will be of 60 kPa. For the driven (C1) pile, this value may be assumed as a lower limit.

7. Conclusions

The analysis of the pile head load-settlement curves of the static load tests of E9 and T1 Piles, using the Modified Two Straight Lines Method (MDRM), led to consistent results with those inferred from the extensometer measurements.

The theoretical relationships between shaft and toe resistances and displacement, derived from the MDRM model, agreed very well with the measured values. For bored (E9) and CFA (T1) piles, the ultimate unit shaft resistance was estimated as 60 kPa. Moreover, the ultimate shaft loads and the toe loads for a 100 mm top settlement were estimated in around 700 kN and 500 kN, respectively, for both E9 and T1 piles, which are in close agreement with the values from a distinct analysis reported by Fellenius *et al.* (2007).

As far as the toe's residual loads are concerned, the estimated values of about 150 kN for the E9 and T1 piles are very much consistent with the measured values (inferred from the tests results), but very much distinct from the "best guess" values reported by Fellenius *et al.* (2007).

For the driven pile (C1), the application of MDRM model assuming two extreme hypothesis, necessary, due to the absence of experimental data to estimate μ, an upper bound value of 500 kN was obtained for the residual load and a lower bound of 500 kN and 60 kPa were derived for the total ultimate and ultimate unit shaft resistances, respectively.

Acknowledgements

The authors are grateful to the Sponsors: Mota-Engil, S.A., Sopecate, S.A.; Tecnasol-FGE, S.A., and Teixeira Duarte, S.A.. This work was developed under the research activities of CEC from the FEUP and ICIST of IST, supported by funding from FCT (Portuguese Science and Technology Foundation). The authors are also indebted to the Polytechnic School of the University of São Paulo, Brazil, for the incentives towards this research.

References

Baguelin, F. & Venon, V.P. (1972) Influence de la compressibilité des pieux sur la mobilizations des éfforts resistant. Bulletin des Liaison Lab. des Ponts et Chaussées. Num. Especial pour les Journées Nationales sur le thème "Le Comportmenet des Sols Avant la Rupture", pp. 308-322.

CFEM (1992). Canadian Foundation Engineering Manual. 3rd ed. Canadian Geotechnical Society, BiTech Publishers, Vancouver, 512 p.

Costa Esteves, E.F.M. (2005) Testing and Analysis of Axially Loaded Piles in a Residual Soil of Granite. M.Sc. Thesis, Faculty of Engineering of the University of Porto, Porto (in Portuguese), 322 p.

Fellenius, B.H. (2001) From strain measurements to load in an instrumented pile. Geotechnical News Magazine, v. 19:1, pp. 35-38.

Fellenius, B.H. (1989) Tangent modulus of piles determined from strain data. Kulhawy, F.H. (ed), The American Society of Civil Engineers, Geotechnical Engineering Division, the 1989 Foundation Congress, v. 1, pp. 500-510.

Fellenius, B.H. (2002a) Basics of Foundation Design. Electronic edition, www.Geoforum.com, 250 p.

Fellenius, B.H. (2002b) Determining the true distribution of load in piles. Proc. International Deep Foundation Congress, An International Perspective on Theory, Design, Construction, and Performance, Orlando, v. 2, pp. 1455-1470.

Fellenius, B.H.; Santos, J.A. & Viana da Fonseca, A. (2007) Analysis of piles in a residual soil - The ISC'2 prediction. Canadian Geotechnical Journal, accepted for publication in v. 1 (January).

Fioravante, V.; Ghionna, V.N.; Jamiolkowski, M. & Pedroni, S. (1995) Load carrying capacity of large diameter bored piles in sand and gravel. Proc. Tenth Asian Regional Conference on Soil Mechanics and Foundation Engineering, pp. 1-13.

Massad, F. (1992) On the interpretation of pile load tests, considering the residual point load and the reversion of the lateral resistance (in Portuguese). Technical Bulletin, Department of Structures and Foundation Engineering, EPUSP, N. BT-PEF 9202. Republished in Solos e Rochas, v. 15:2, pp. 103-115.

Massad, F. (1995) Pile analysis taking into account soil rigidity and residual stresses. Proc. Xth Panamerican Congress on Soil Mechanics and Foundation Engineering, Guadalahara, v. 2, pp. 1199-1210.

Lazo, G. (1996) Prediction of the Behaviour of Precast Piles in S. Paulo Large Region, Brazil, by Means of Mathematical Models. MSc Thesis, EPUSP, University of São Paulo, São Paulo, 222 p.

Massad, F. & Lazo, G. (1998) Graphical method for the interpretation of the load-settlement curve from vertical load tests on rigid and short piles. Proc. XI Brazilian Congress on Soil Mechanics and Geotechnical Engineering, Brasília, v. 3, pp. 1407-1414.

Marques, J.A.F. & Massad, F. (2004) Load tests on instrumented bored piles with bulbs, executed at a seafront in Maceió, Alagoas. Solos e Rochas, v. 27:3, pp. 243-260 (in Portuguese).

Santos, J.S.; Viana da Fonseca, A. & Costa Esteves, E. (2006) ISC'2 experimental site - Prediction & performance of instrumented axially loaded piles. Geotecnia, n. 107, pp. 79-90 (in Portuguese).

Santos, J.A.; Leal Duarte, R.; Viana da Fonseca, A.; Costa Esteves, E. (2005) ISC'2 experimental site - Prediction & performance of instrumented axially loaded piles. Proc. 16th ICSMFE, Osaka, v. 4, pp. 2171-2174.

Viana da Fonseca, A. (2003) Characterizing and deriving engineering properties of a saprolitic soil from granite, in Porto. Tan *et al.*, (eds) Characterization and Engineering Properties of Natural Soils. Swets & Zeitlinger, Lisse, pp. 1341-1378.

Viana da Fonseca, A. & Almeida e Sousa, J. (2001) At rest coefficient of earth pressure in saprolitic soils from granite. Proc. XIV ICSMFE, Istambul, v. 1, pp. 397-400.

Viana da Fonseca, A. & Ferreira, C. (2000) Management of sampling quality on residual soils and soft clayey soils. Comparative analysis of in situ and laboratory seismic waves velocities. Proc. Workshop Sampling Techniques for Soils and Soft Rocks & Quality Control, FEUP, Porto, pp. 3-75 (in Portuguese).

Viana da Fonseca, A. & Ferreira, C. (2002) The application of the Bender Elements technique on the evaluation of sampling quality of residual soils. Proc. XII COBRAMSEG, ABMS, São Paulo, v. 1, pp. 187-199 (in Portuguese).

Viana da Fonseca, A.; Carvalho, J.; Ferreira, C.; Tuna, C.; Costa, E. & Santos, J. (2004) Geotechnical characterization of a residual soil profile: the ISC'2 experimental site, Porto. Viana da Fonseca, A. & Mayne, P.W. (eds) Geotechnical & Geophysical Site Characterizaton. Millpress, Rotterdam, pp. 1361-1370.

Viana da Fonseca, A.; Carvalho, J.; Ferreira, C.; Santos, J.A.; Almeida, F. & Hermosilha, H. (2005) Combining geophysical and mechanical testing techniques for the investigation and characterization of ISC'2 residual soil profile. Proc. 16th ICSMGE, Osaka, v. 2, pp. 765-768.

Viana da Fonseca, A.; Carvalho, J.; Ferreira, C.; Santos, J.A.; Almeida, F.; Pereira, E.; Feliciano, J.; Grade, J. & Oliveira, A. (2006) Characterization of a profile of residual soil from granite combining geological, geophysical, and mechanical testing techniques. Int. J. Geotechnical and Geological Engineering, v. 24:5, pp. 1307-1348.

Viana da Fonseca, A. & Santos, J. (2006) International Prediction Event on the Behaviour of Bored, CFA and Driven Piles in CEFEUP/ISC'2 Experimental Site - 2003. Final Report. Ed. FEUP, Porto (in press).

List of symbols

A: Cambefort parameter (see Fig. 15)
A_{lr}: ultimate shaft resistance
B: Cambefort parameter (see Fig. 14)
c': effective cohesion
CFA: Continuous Flight Auger (pile)
CH: Cross-Hole test
CPTu: Static Cone Penetrometer Test (u for piezocone)
D: diameter or width of the pile
DMT: Marchetti Flat Dilatometer Test
E: deformability (Young's) modulus
E: modulus of elasticity of the pile material
E_M (E_{pm}): Ménard pressuremeter modulus
E_0: small strain (maximum) deformability (Young's) modulus

f_s: CPT shaft resistance;
f_u: ultimate unit shaft resistance
f_{res}: residual negative shaft resistance
$G_0 = G_{max}$: small strain (maximum) shear modulus
G_l: small strain shear modulus at pile base level
h: height of the pile
k: relative stiffness of the pile-soil (shaft) system
K_r: pile stiffness
K_0: coefficient of earth pressure at rest
N_{SPT}: number of blows in SPT tests
N_{60}: NSPT values for a reference energy ratio of 60%
P_h: residual toe load
p_{LM}: Ménard's net limit pressure
P_o: Pile top load
PMT Pre-bored Ménard Pressuremeter Test
q_c: cone resistance in CPT tests
Q_p: Tip load or resistance
Q_{pr}: ultimate tip load or resistance
Q_{rupt}: ultimate total pile load
R: Cambefort parameter (see Fig. 15)
R_{reb}: Cambefort parameter (see Fig. 15)
R_p: Toe unit resistance
s: settlement
S: pile cross section area
SPT: Standard Penetration Test
SPLT: Static Pile Load Test
V_s: shear wave's velocity
y_o: pile top settlement
y_l: Cambefort parameter (see Fig. 14)
y_{lR}: Cambefort parameter (see Fig. 14)
z: square root of k; depth (from the ground surface)
γ: unit weight
η: correction factor to allow for the pile base depth effects
λ: relative stiffness of the pile-soil (shaft and toe) system
μh: Randolph and Wroth's parameter that has the same meaning as k
ϕ': angle of shearing resistance ("friction angle")
μ: shaft friction magnifier factor due to residual load
ν: Poisson's ratio